

## Synchronization and antisynchronization of chaotic power drop-outs and jump-ups of coupled semiconductor lasers

Immo Wedekind and Ulrich Parlitz\*

*Drittes Physikalisches Institut, Universität Göttingen, Bürgerstraße 42-44, D-37073 Göttingen, Germany*

(Received 8 August 2001; published 28 August 2002)

Experimental observations and numerical simulations of synchronization and antisynchronization of low-frequency power drop-outs and jump-ups of chaotic semiconductor lasers are presented.

DOI: 10.1103/PhysRevE.66.026218

PACS number(s): 42.55.Px, 05.45.Xt

During the last decade, synchronization of chaotic systems has been explored very intensively in various fields ranging from physics and mathematics to engineering and biology [1]. The strong interest in different features of chaotic synchrony was partly motivated by potential applications in communication systems. In particular, optical systems have been studied because of their important role in modern communication devices. There, synchronization of chaotic lasers was first observed with Nd:YAG (Nd: yttrium aluminum garnet) and CO<sub>2</sub> lasers [2]. Later, synchronization of chaotic erbium-doped fiber ring lasers was studied in detail theoretically [3] and experimentally [4], where also messages were encoded in the chaotic dynamics and subsequently recovered in the receiver.

For technical applications in communication systems semiconductor lasers are of particular interest, because they are compact and can easily be modulated [5,6]. Chaos in semiconductor lasers arises in different ways: due to (periodic) modulation of the pump current [7], due to electro-optical feedback where the pump current is modulated by the emitted light intensity [8,9], or due to an external cavity (optical feedback) [10]. In several cases it turned out to be possible to synchronize the chaotic fluctuations of the intensity of the emitted light by means of suitable coupling schemes. A communication scheme based on synchronization of chaotic laser diodes with electro-optical feedback was implemented experimentally by Goedgebuer *et al.* [11]. Recently, Chen and Liu simulated successfully information transmission using optical feedback [12].

All optical feedback in external cavity semiconductor lasers (ECSLs) has been a subject of extensive research during the last 15 years because of its importance in technical applications such as optical data storage or optical fiber communications [13]. In most of these cases, effects due to optical feedback are unwanted and engineers try to avoid them.

A typical phenomenon occurring in ECSLs are low frequency fluctuations (LFFs), where the intensity of the emitted light oscillates in the 5–10 GHz range with an envelope that shows relatively slow, irregular fluctuations (about 10 MHz). These slow fluctuations are either power drop-outs or power jump-ups as illustrated in Fig. 1.

Power drop-outs have been studied very much in detail during the last 15 years [14,15] and are usually meant when

the phenomenon of LFFs is addressed. In particular, the question whether the underlying dynamics is (mainly) a stochastic process or governed by a chaotic attractor has been discussed controversially [16–19]. Numerical simulations based on a deterministic model [20] indicate that LFF dynamics is governed by a very high-dimensional chaotic attractor and is thus very difficult to distinguish from a stochastic signal, a feature that makes them interesting candidates for an optical encryption system.

For high pump currents and high reflectivity of the mirror of the external cavity power jump-ups occur [Fig. 1(b)] that have first been reported by Pan *et al.* [21], but have not been investigated further since then.

Synchronization of low frequency power drop-outs has been shown first numerically by Ahlers *et al.* [20] simulating a pair of unidirectionally injection coupled semiconductor lasers as shown in Fig. 2. Soon after this successful simulation, synchronization was also demonstrated experimentally by Takiguchi *et al.* [22] and Sivaprakasam and Shore [23]. Figure 3(a) shows an experimental example for synchronization of this kind of LFFs.

Depending on the coupling the phenomenon of “anticipation” of chaos synchronization [24] may occur where the intensity fluctuations of the response laser run ahead the output of the drive [25].

Only recently it was demonstrated experimentally that not only synchronization of power drops can be achieved but also antisynchronization where the intensity of the response laser jumps up when the drive intensity drops [26,27], as shown in Fig. 3(b). Switching between both types of synchronization is possible, for example, by changing slightly

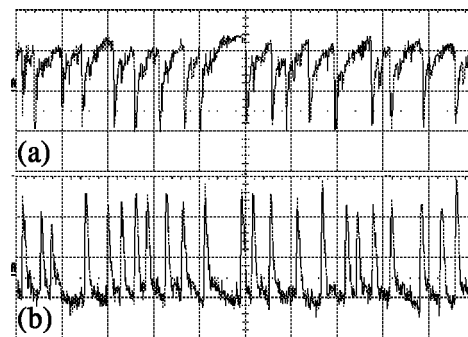


FIG. 1. Intensity (in arbitrary units) vs time for an ECSL showing low frequency fluctuations: (a) power drop-outs (time scale 0.1  $\mu$ s/div), (b) power jump-ups (time scale 0.2  $\mu$ s/div).

\*Email address: parlitz@dpi.physik.uni-goettingen.de

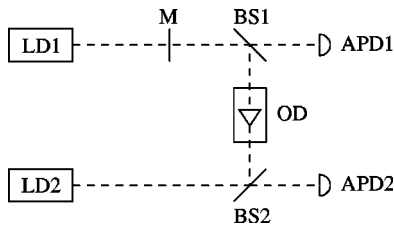


FIG. 2. Setup of unidirectionally injection coupled external cavity semiconductor lasers studied in this paper. The size of the external cavity is about 40 cm [LD, laser diode (*Mitsubishi ML 1412R*); M, mirror; BS, nonpolarizing beam splitter; OD, optical diode (*Faraday isolator Optics for Research IO-635-HP*); APD, avalanche photodiode].

the pump current of the drive system [26]. This feature may also be of importance for potential applications in communication systems.

In this paper we present experimental observations of (anti)synchronization of low frequency power jump-ups as shown in Figs. 3(c) and 3(d). The drive laser produces irregular jump-ups and the response laser follows these jump-ups [synchronization, Fig. 3(c)] or shows synchronized power drop-outs [Fig. 3(d)] that we call antisynchrony.

In order to answer the question where in parameter space (anti)synchronization occurs we have systematically varied the pump currents and temperatures of both unidirectionally coupled lasers. To monitor synchronization, intensity time series of both the drive and the response laser have been sampled by means of an avalanche photodiode (see Fig. 2). For each data set a *synchronization index*  $S$  was computed as the product of the peak-to-peak-amplitude of the response laser intensity and the largest cross correlation of both signals. Vanishing values of the synchronization index indicate lack of any synchronization, large positive values correspond to synchronization and negative values of large magnitude occur for antisynchronization. Weighting the linear correlation by the response amplitude turned out to be necessary to avoid spurious results, because outside the synchronization regime the intensity of the response laser is so weak that random fluctuations due to discretization errors may indicate artificial correlations.

Figure 4 shows four phase diagrams where the synchronization index  $S$  is plotted grayscaled versus pump current and temperature of one of the lasers (the pump current and temperature of the other laser are kept fixed). Figure 4(a) shows the synchronization diagram for the case where the drive laser displays low frequency power drop-outs and the pump current  $I_2$  and temperature  $T_2$  of the response laser are varied. The almost horizontal white and black stripes correspond to regions where synchronization or antisynchronization occurs, respectively. A similar pattern is found when varying the pump current  $I_1$  and the temperature  $T_1$  of the drive laser while keeping the parameters of the response laser fixed [Fig. 4(b)]. Figures 4(c) and 4(d) show corresponding results for low frequency jump-up dynamics of the driving laser.

In order to model the observed synchronization phenomena we used the well-known Lang-Kobayashi equations [28] for the electron population  $N$  and the slowly varying com-

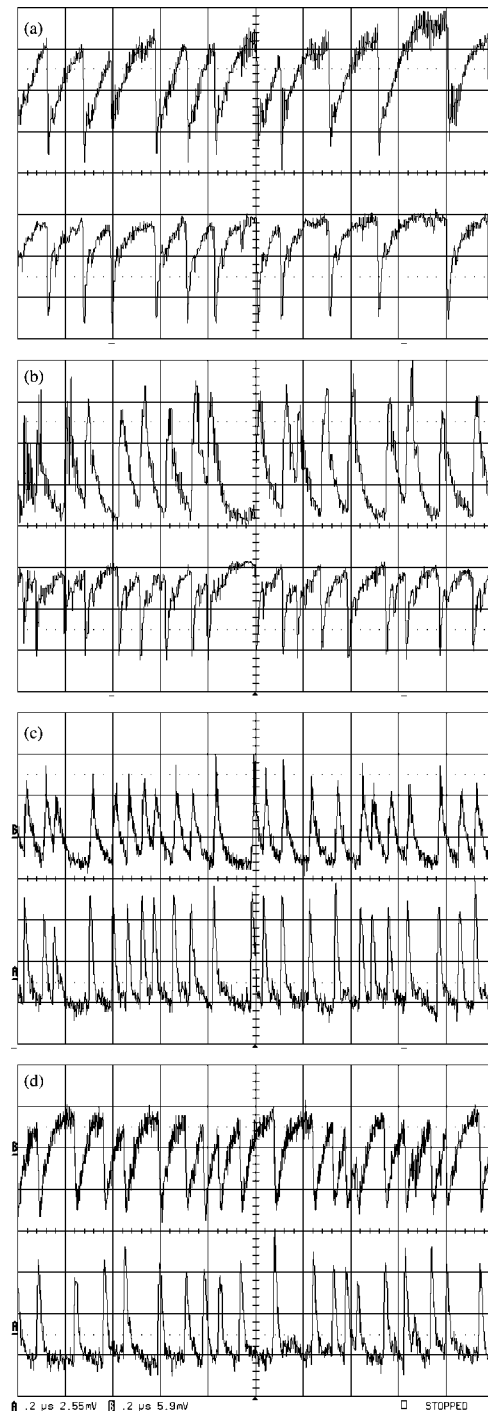


FIG. 3. Experimental observation of synchronization and anti-synchronization of low frequency fluctuations of the light intensity (in arbitrary units). The lower and upper traces in each part correspond to drive and response, respectively. (a) power drop-outs, synchronization (time scale  $0.1 \mu\text{s}/\text{div}$ ); (b) power drop-outs: anti-synchronization (time scale  $0.1 \mu\text{s}/\text{div}$ ); (c) power jump-ups, synchronization (time scale  $0.2 \mu\text{s}/\text{div}$ ); (d) power jump-ups, anti-synchronization (time scale  $0.2 \mu\text{s}/\text{div}$ ).

plex amplitude  $E(t)$  of the intracavity optical field oscillating at the angular frequency  $\omega_0$ . These equations are generally considered to give a valid approximation of a single mode SL with weak to moderate optical feedback from an external

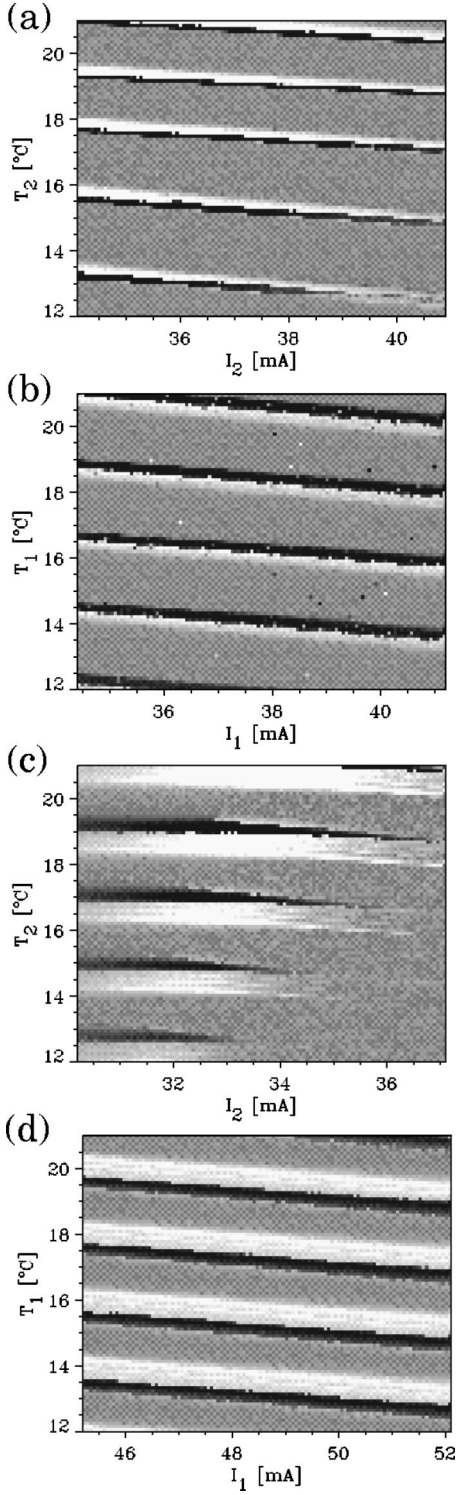


FIG. 4. Synchronization index  $S$  (grayscaled) vs pump current  $I$  and temperature  $T$  of drive (index 1) or response (index 2) laser. White indicates synchronization and black indicates antisynchronization. (a) drive laser, power drop-outs,  $S$  vs  $(I_2, T_2)$  for  $I_1 = 34.4$  mA and  $T_1 = 19.5^\circ$  C. (b) drive laser: power drop-outs,  $S$  vs  $(I_1, T_1)$  for  $I_2 = 37.8$  mA and  $T_2 = 19.5^\circ$  C. (c) drive laser, power jump-ups,  $S$  vs  $(I_2, T_2)$  for  $I_1 = 46$  mA and  $T_1 = 19.5^\circ$  C. (d) drive laser, power jump-ups,  $S$  vs  $(I_1, T_1)$  for  $I_2 = 33$  mA and  $T_2 = 19.5^\circ$  C.

resonator,

$$\frac{d}{dt}E(t) = \frac{1}{2}\{-i\alpha G_N[N(t) - N_{sol}] + [G(N) - \Gamma]\}E(t) + \kappa E(t - \tau)e^{i\omega_0\tau},$$

$$\frac{d}{dt}N(t) = pJ_{th} - \gamma N(t) - G(N)|E(t)|^2,$$

$$\frac{d}{dt}\tilde{E}(t) = \frac{1}{2}\{-i\alpha G_N[\tilde{N}(t) - N_{sol}] + [G(\tilde{N}) - \Gamma]\}\tilde{E}(t) + \rho\langle E(t - \tau_c)e^{i(\omega_0\tau_c + \Delta\omega_0 t)}, e^{i\varphi} \rangle e^{i\varphi}, \quad (1)$$

$$\frac{d}{dt}\tilde{N}(t) = \tilde{p}J_{th} - \gamma\tilde{N}(t) - G(\tilde{N})|\tilde{E}(t)|^2.$$

The delay  $\tau_c$  due to coupling depends on the distance between both lasers and was chosen to equal zero in the simulations. The meaning and values of other parameters are given in Table I.

The second laser system possesses no external cavity. The difference between the emitted light frequencies of both lasers  $\Delta\omega_0$  leads to a modulation  $e^{i\Delta\omega_0 t}$  of the coupling term in Eq. (1).

The polarization due the Faraday isolator used for unidirectional coupling (see Fig. 2) is modeled by a scalar product

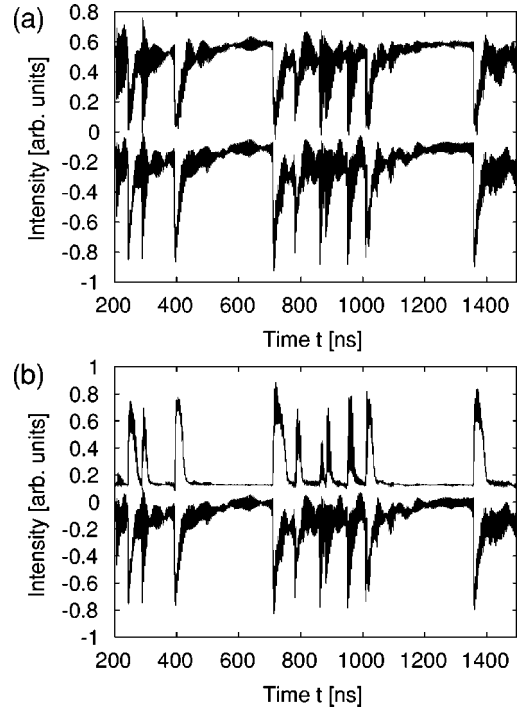


FIG. 5. Numerical simulation of (a) synchronization and (b) antisynchronization of low frequency power drop-outs. For comparison with the experimentally measured intensities the signals are low-pass filtered (500 MHz). The lower and upper traces in each part correspond to drive and response, respectively.

TABLE I. Parameters used in the simulations, values taken from Ref. [21].

Solitary laser carrier number	$N_{sol}$	$5.9 \times 10^8$
Differential optical gain	$G_N$	$3.5 \times 10^3 \text{ s}^{-1}$
External cavity round trip time	$\tau$	4 ns
Linewidth enhancement factor	$\alpha$	3.0
Stimulated emission rate	$G$	$\approx G_N[N - N_{sol}]$
Carrier decay rate	$\gamma$	$5.29 \times 10^8 \text{ s}^{-1}$
Cavity decay rate	$\Gamma$	$7.14 \times 10^{11} \text{ s}^{-1}$
Reflection coefficient	$\kappa$	$1.75 \times 10^{11}$
Coupling coefficient	$\sigma$	$5 \times 10^{11}$
Laser threshold current	$J_{th}$	$3.12 \times 10^{17} \text{ s}^{-1}$
Wavelength	$2\pi c/\omega_0$	635 nm

$\langle \cdot, \cdot \rangle$  of the transmitted electrical field with  $e^{i\varphi}$  in the coupling term where  $\varphi$  stands for the angle of the output of the polarizer.

Figure 5 shows simulated synchronization [Fig. 5(a)] and antisynchronization [Fig. 5(b)] of low-frequency drop-outs.

Without polarization term in the coupling we did not succeed in simulating antisynchronization. Similar results for power jumps-ups in the drive laser have not been simulated yet because the Lang-Kobayashi delay differential equations are not appropriate for (very) high reflection coefficients which are necessary to generate *autonomous* power jumps in the driving laser. Another challenge is the proper explanation of the physical mechanisms underlying the phenomena of synchronization and antisynchronization. The occurrence of “stripes” of (anti)synchronization in Fig. 3 may be explained by changes of the wavelength when varying pump current or temperature, but a complete model is still absent.

## ACKNOWLEDGMENTS

We thank C. Massoller, R. Roy, H. D. I. Abarbanel, and the members of our nonlinear dynamics group for stimulating discussions on chaos synchronization in semiconductor lasers. Furthermore, we thank K. Lautscham, W. Ebrecht, and H. Hohmann for technical assistance and the BMBF (13N7979) for financial support.

- 
- [1] Chaos **7** (1997); IEEE Trans. Circuits Syst. **44**, (1997); *Handbook of Chaos Control*, edited by H. G. Schuster (Wiley-VCH, Weinheim, 1999).
- [2] R. Roy and K.S. Thornburg, Phys. Rev. Lett. **72**, 2009 (1994); T. Sugawara, M. Tachikawa, T. Tsukamoto, and T. Shimizu, *ibid.* **72**, 3502 (1994); P. Colet and R. Roy, Opt. Lett. **19**, 2056 (1994).
- [3] H.D.I. Abarbanel and M.B. Kennel, Phys. Rev. Lett. **80**, 3153 (1998).
- [4] G.D. VanWiggeren and R. Roy, Science **279**, 1198 (1998); Phys. Rev. Lett. **81**, 3547 (1998).
- [5] G. P. Agrawal and N. K. Dutta, *Semiconductor Lasers*, 2nd ed. (Van Nostrand Reinhold, New York, 1993).
- [6] G.H.M. van Tartwijk and D. Lenstra, Quantum Semiclass. Opt. **7**, 87 (1995).
- [7] J. Sacher *et al.*, Phys. Rev. A **45**, 1893 (1992).
- [8] C.-H. Lee and S.-Y. Shin, Appl. Phys. Lett. **62**, 922 (1993).
- [9] S.I. Turovets, J. Dellunde, and K.A. Shore, J. Opt. Soc. Am. B **14**, 200 (1997).
- [10] J. Mørk, B. Tromborg, and J. Mark, IEEE J. Quantum Electron. **28**, 93 (1992).
- [11] J.-P. Goedgebuer, L. Larger, and H. Porte, Phys. Rev. Lett. **80**, 2249 (1998).
- [12] H.F. Chen and J.M. Liu, IEEE J. Quantum Electron. **36**, 27 (2000).
- [13] I. Fischer, G.H.M. van Tartwijk, A.M. Levine, W. Elsässer, E. Göbel, and D. Lenstra, Phys. Rev. Lett. **76**, 220 (1996); I. Fischer, T. Heil, M. Münkel, and W. Elsässer, Proc. SPIE **3283**, 63 (1998).
- [14] H. Tempin, N.A. Olsson, J.H. Abeles, R.A. Logan, and M.B. Panish, IEEE J. Quantum Electron. **22**, 286 (1986).
- [15] T. Sano, Phys. Rev. A **50**, 2719 (1994).
- [16] J. Sacher, W. Elsässer, and E.O. Göbel, Phys. Rev. Lett. **63**, 2224 (1989).
- [17] T. Sano, Phys. Rev. A **50**, 2719 (1994).
- [18] G.H.M. van Tartwijk, A.M. Levine, and D. Lenstra, IEEE J. Sel. Top. Quantum Electron. **1**, 466 (1995).
- [19] C.H. Henry and R.F. Kazarinov, IEEE J. Quantum Electron. **QE-22**, 294 (1986); A. Hohl, H.J.C. van der Linden, and R. Roy, Opt. Lett. **20**, 2396 (1995); M. Giudici, C. Green, G. Giacomelli, U. Nespolo, and J.R. Tredicce, Phys. Rev. E **55**, 6414 (1997); D.W. Sukow, J.R. Gardner, and D.J. Gauthier, Phys. Rev. A **56**, R3370 (1997).
- [20] V. Ahlers, U. Parlitz, and W. Lauterborn, Phys. Rev. E **58**, 7208 (1999).
- [21] M.-W. Pan, B.-P. Shi, and G.R. Gray, Opt. Lett. **22**, 166 (1997).
- [22] Y. Takiguchi, H. Fujino, and J. Ohtsubo, Opt. Lett. **24**, 1570 (1999).
- [23] S. Sivaprakasam and K.A. Shore, Opt. Lett. **24**, 466 (1999); S. Sivaprakasam, E.M. Shahverdiev, and K.A. Shore, Phys. Rev. E **62**, 7505 (2000).
- [24] H.U. Voss, Phys. Rev. E **61**, 5115 (2000).
- [25] C. Masoller, Phys. Rev. Lett. **86**, 2782 (2000).
- [26] I. Wedekind and U. Parlitz, Int. J. Bifurcation Chaos Appl. Sci. Eng. **11**, 1141 (2001).
- [27] S. Sivaprakasam, I. Pierce, P. Röss, P.S. Spencer, and K.A. Shore, Phys. Rev. A **64**, 013805 (2001).
- [28] R. Lang and K. Kobayashi, IEEE J. Quantum Electron. **QE-16**, 347 (1980).